International Journal of Theoretical Physics, Vol. 42, No. 4, April 2003 (© 2003)

Contribution of J-Dependent Potential in Differential Cross-Sections of Two-Nucleon Transfer Reactions

A. A. Farra[1]

Received November 11, 2002

Heavy-ion reactions with two-nucleon transfer are studied within the framework of the distorted wave Born approximation (DWBA) calculations. The bound-states of the transferred particle with the core nucleus forming the projectile or target and residual nuclei are represented by a Yukawa potential. The calculated differential cross-sections are in good agreement with the experimental data. The study exhibits the important contributions of the J-dependent potential in reproducing the large-angle oscillatory structures of two-nucleon transfer reactions.

KEY WORDS: J-dependent potential; two-nucleon transfer reactions.

1. INTRODUCTION

The two-nucleon transfer reactions have been studied using the DWBA calculations at energies below and above the Coulomb barrier (Maglione *et al.*, 1985; Videback *et al.*, 1985). The oscillatory structures of the differential cross-sections of two-nucleon transfer reactions have been well described using both Coupled Channel Born approximation (CCBA) and DWBA calculations (Kondo and Tamura, 1984). Recently the uprising oscillatory structures of heavy-ion transfer reactions (Gao *et al.*, 1988; Xia and He, 1988) were investigated in terms of the nuclear molecular-orbital theory. In such calculations, although the DWBA calculations (Kabir *et al.*, 1988) show a wide discrepancy to the backward angle data, but a reasonable investigations have been achieved within the density-dependent calculations (Ferrero *et al.*, 1990), parity-dependent potential (Bilwes *et al.*, 1987), and real-folding potential (Charaji *et al.*, 1993; Treka *et al.*, 1990).

In the present work, the differential cross-sections of heavy-ion reactions with two-particle transfer have been calculated using DWBA calculations as a single direct-step process. The nucleus–nucleus interaction is taken to have real

[1] Physics Department, Faculty of Science, Al-Azhar University, Gaza, Palestine.

0020-7748/03/0400-0881/0 © 2003 Plenum Publishing Corporation

and imaginary Woods-Saxon form. The obtained results of the present theoretical DWBA calculations are fitted to the experimental data to extract the corresponding spectroscopic factors.

In Section 2, first-order DWBA formulation is introduced. Numerical calculations and results are given in Section 3. Section 4 is left for discussion and conclusions.

2. FIRST-ORDER DWBA APPROACH

In this section, we deal with a one-step distorted wave Born approximation process (Tamaura, 1974). Therefore, the transition matrix element T_{fl} for heavy-ion transfer reaction $T(A, X)R$ with a transferred particle C is expressed to have the post form

$$T_{fl} = \sum_{\substack{lj \\ l'j'}} S(l, j)S^*(l', j')\langle J_X\mu_X; (J_C j'(J_A l')) | T^{ll'} | J_T\mu_T; J_A\mu_A(J_C j(J_X l)) \quad (1)$$

where $S(l, j)$ and $S^*(l', j')$ are the spectroscopic factors in the initial and final channels, respectively; J_i and μ_i are the spin angular momentum of the particle i and its magnetic projection on the z-component; $T^{ll'}$ is the reduced transition matrix element, given as

$$T^{ll'} = \int F(r)\phi_{TC}^{*l'j'}(\vec{r}_{TC})\psi_{XR}^{*(-)}\left(\vec{K}_X, -\frac{M_T}{M_R}\vec{r}_{TC}\right)\psi_{AT}^{(+)}(\vec{K}_A, \vec{r}_{TC})d\vec{r}_{TC} \quad (2)$$

where $\psi_{AT}^{(+)}$ and $\psi_{XR}^{(-)}$ are the ingoing and outgoing distorted wave functions, while $\phi^{l'j'}$ stands for the wavefunction which describes the bound state of the residual nuclei R; F(r) is the reduced form factor expressed as

$$F(r) = V_{xc}^0 N(l, \ldots)_{(2l+1)} e^{\frac{R_X+R_C}{a}} \cdot \left[\frac{Z}{2a} + \frac{1}{\sqrt{\pi}}\left(1 - \frac{R_x + R_c}{2a}\right)(Z^2 + Q^2) \cdot \frac{1}{(Z^2 + Q^2)^2}\right] \quad (3)$$

where

$$Z = \beta + \frac{1}{a} \quad (4)$$

and

$$Q^2 = (\sigma' E_f + \gamma' E_i - \delta' E_{TC}^{bin}) + (\delta' V_{TC}(r_{TC}) - \gamma' \tilde{V}_i(r_{TC}) - \sigma' \tilde{V}_f(r_{TC})) \quad (5)$$

The statistical factors σ', γ', and δ' are adjusted within the local WKB-approximation to have the values

$$\sigma' = 2\sigma\frac{m_{XR}}{\hbar^2}, \qquad \gamma' = 2\gamma\frac{m_{AT}}{\hbar^2} \quad \text{and} \quad \delta' = 2\delta\frac{m_{AT}}{\hbar^2} \quad (6)$$

where the coefficients σ, γ, and δ are expressed to have

$$\sigma = 1 + \frac{M_X}{M_A}, \qquad \gamma = \frac{M_X}{M_A}\left(1 + \frac{M_X}{M_A}\right) \quad \text{and} \quad \delta = \frac{-M_X}{M_A} \tag{7}$$

M_{ij} is the reduced mass of the particles i and j; where E_i, E_f, and E_{TC} are the respective initial, final, and binding energies; $\tilde{V}_i$ and $\tilde{V}_f$ are the optical potentials in the initial and final channels, respectively, while V_{TC} stands for the bound-state interaction in the final channel which is taken to have Yukawa plus exponential potential (Sikora *et al.*, 1980).

$$V_{ij}(r_{ij}) = V^0\left(2 + \frac{r_{ij} - (R_i + R_j)}{a}\right) e^{\frac{-r_{ij}+R_i+R_j}{a}} \tag{8}$$

where

$$V^0 = [C(i)C(j)]^{\frac{1}{2}} \frac{a R_i R_j}{r_0^2(R_i + R_j)} \tag{9}$$

and the parameter $C(p)$ has the value

$$C(p) = A(p)\left[1 - K_s\left(\frac{N_p - Z_p}{A_p}\right)^2\right]; \quad p = i, j \tag{10}$$

In these calculations, the bound-state wave function $\phi_{ij}(\vec{r}_{ij})$ is taken to have Morinigo form

$$\phi_{ij}(\vec{r}_{ij}) = N(l, \ldots)\, e^{-\beta r_{ij}} r_{ij}^{l-1} Y_m^l(\hat{\vec{r}}_{ij}) \tag{11}$$

where

$$N(l, \ldots) = \left(\frac{(2\beta)^{2l+1}}{(2l)!}\right)^{\frac{1}{2}} \tag{12}$$

and

$$\beta^2 = \frac{2m_{ij}}{\hbar^2}|E_{ij}^{bin}|. \tag{13}$$

3. NUMERICAL CALCULATIONS AND RESULTS

In this section, numerical calculations are carried out for different heavy-ion reactions with two-nucleon transfer. In the calculations presented in this section, we consider ^{16}O(^{6}Li,α)^{18}F and ^{76}Ge(^{16}O, ^{14}C)^{76}Se. In a first set of calculations, the optical potential is taken to have the standard Woods-Saxon potential (Kondo

Table I. Woods-Saxon Optical Potential Parameters

Channel	Set	V_0 (MeV)	r_v (fm)	a_v (fm)	W_0 (MeV)	r_w (fm)	a_w (fm)	r_c (fm)	Refs.
^{4}He + ^{19}F	I	180.0	1.42	0.56	16.5	1.42	0.56	1.40	Lepine-Szily *et al.*, 1990
	II	170.0	1.26	0.78	12.0	1.85	0.85	1.25	
^{6}Li + ^{16}O	I	187.0	1.30	0.70	31.4	1.70	0.90	1.40	Tanabe *et al.*, 1981
	II	160.6	1.25	0.79	9.0	2.05	0.85	1.35	
^{16}O + ^{76}Ge	I	100.1	1.06	0.63	24.0	1.20	0.62	1.06	Humanic *et al.*, 1982
^{14}C + ^{78}Se	I	85.40	1.22	0.49	39.2	1.20	0.47	1.25	
	II	40.0	1.34	0.45	25.0	1.50	0.45	1.45	

and Tamura, 1984) together with a Coulomb potential. The potential used is expressed as

$$\tilde{V}(r) = -V_0\{1 + \exp[(r - R_v)/a_v]\}^{-1} - iW_0\{1 + \exp[(r - R_w)/a_w]\}^{-1} + V^{\mathrm{C}}(r) \tag{14}$$

$V^{\mathrm{C}}(r)$ is the Coulomb potential due to a uniform charge sphere of radius $R_C = r_c A^{1/3}$ fm. The interaction radii have the expression

$$R_x = r_x\left(A_i^{1/3} + A_j^{1/3}\right) \quad \text{for } x = v, w, c. \tag{15}$$

For numerical calculations, the parameters of the optical potential are expressed in different sets to investigate the sensitivity contribution of these parameters in reproducing the experimental data as listed in Table I. Whereas the different parameters of Yukawa interaction are given as $A(i) = 21.17$ MeV, $r_0 = 1.18$ fm, $a = 0.65$ fm, and the surface a symmetry constant $K_{\mathrm{S}} = 3.0$ which are chosen to fit the static properties of nuclei. The bound-state parameters are taken as those used in the previous calculations given in Table II. The number of nodes of the radial wave functions are calculated from the harmonic oscillator relation. Initially, the present DWBA calculations were performed using the Woods-Saxon potential parameters (Set I). It is found that the parameters Set I provide a reasonable description of the forward angle region, but they do not fit the large angle data. Therefore, the

Table II. Bound-State Parameters

State	E (MeV)	$r_0{}^a$ (fm)	a (fm)
^6L_i=^{4}He ⊕ d (1^+ g.s.; 2s and 1d)	1.47	1.05	0.65
^{16}O=^{12}C ⊕ ^{4}He (0^+ g.s.; 2s)	7.16	1.20	0.60
^{18}F=^{16}O + d (1^+ g.s.; 2s, 3s, and 2d)	7.53	1.29	0.65
(3^+ 0.927 MeV; 2d)			
(5^+ 1.022 MeV; 1g)			
^{18}F=^{12}C + ^{6}L$_i$ (1^+ g.s.; 4s and 3d)	13.22	1.20	0.60

$^a R_{\mathrm{bound}} = \mathrm{r}_0\,(A_1^{1/3} + A_2^{1/3})$ fm.

six-potential parameters are varied to obtain the best fit of the data. The resulting parameters are listed in Table I in different families (Set II). Generally, it is found that the obtained parameters are not drastically different from those used to start searches. In this analysis, the parameters of the model are varied to give the best fit to the data by minimizing

$$\chi^2 = \sum_{i=l}^{n} \left(\frac{\sigma_{\exp}(\theta_i) - \sigma_{\text{theo}}(\theta_i)}{\Delta\sigma_{\exp}(\theta_i)} \right)^2 \tag{16}$$

where n is the number of the differential cross-section data points, $\sigma_{\text{theo}}(\theta_i)$ being the i-th calculated cross-sections, $\sigma_{\exp}(\theta_i)$ and $\Delta\sigma_{\exp}(\theta_i)$ are the corresponding experimental cross-sections and their relative uncertainties. The results of the present numerical calculations of the form factors are introduced in Figs. 1 and 2. In general, the form factors behave in a typical behavior and yield nearly the same shapes for all mentioned states. However, the results obtained for the differential cross-sections are given in Figs. 3 and 4 as shown by the dashed lines. The fits to the data are quite good over the entire angular range but the predictions are too low in magnitude at large angles for the most considered states.

In an effort to investigate the sensitivity of the differential cross-sections to the details of the ion–ion interactions, the optical potential model is modified to include different absorptions. In these calculations the imaginary potential is demonstrated by the superiority of angular momentum-dependent absorptive from Kondo *et al.* (1985) given as

$$W(r, j) = W_0(1 + \exp[(r - R_w)/a_w])^{-1}(1 + \exp[(J - J_c)/\Delta J])^{-1} \tag{17}$$

where J_c is a cutoff angular momenta and ΔJ is the angular momenta cutoff diffuseness parameter. For each energy J_c is parameterized by the expression

$$J_c = \bar{R}[(2\mu/\hbar^2)(E_{cm} - \bar{Q})]^{\frac{1}{2}} \tag{18}$$

where $\bar{R}$ and $\bar{Q}$ represent average values of the radius and the threshold energy for the predominant nonelastic reactions, respectively; μ is the reduced mass of the system. In fact, although the calculated differential cross-sections with J-dependent imaginary potential (solid lines) are comparable to those using real and imaginary Woods-Saxon form factors (WS + WS) at forward angles but are quite different at large angles. As shown in Figs. 3 and 4, it is found that the effect of J-dependent potential is small in the backward region. Generally, calculations employing Woods-Saxon potential fit reasonably well the forward angle data but give rise back angle. However, the inclusion of the J-dependent potential improves the cross-section magnitudes and exhibits good results better than those using standard Woods-Saxon potentials. In comparison, using both (WS + WS) and (WS + JD) optical potentials are found to be in a good agreement with the experimental data

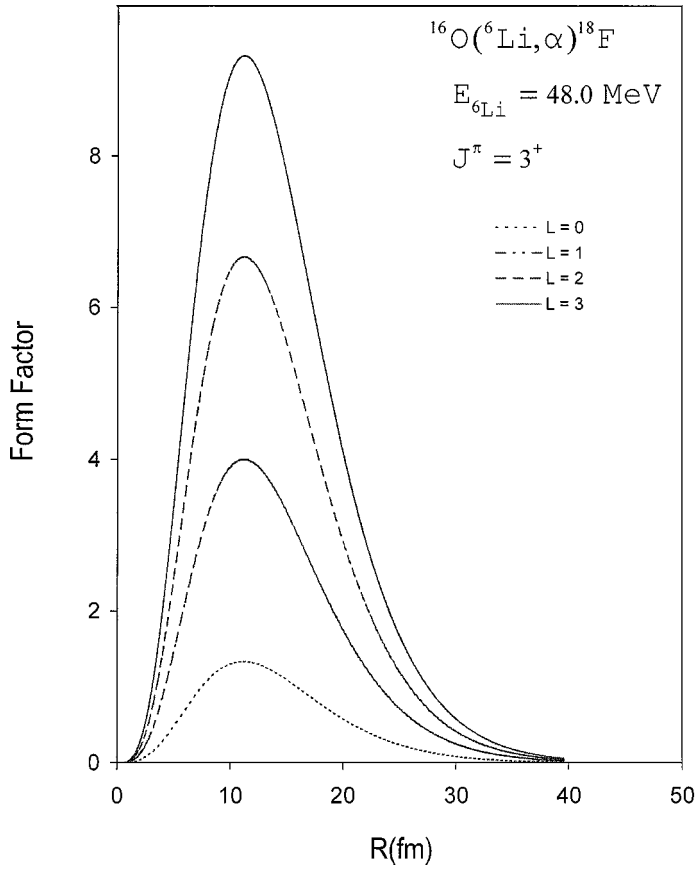

Fig. 1. Yukawa form factors of $^{16}O(^{6}Li, \alpha)^{18}F$ reaction for different angular momenta with optical potential parameters (Set II).

in the forward region. In addition, although calculations employing J-dependent imaginary potentials give an equivalent fit to the experimental data in the large angle region as shown in Fig. 4 but it grossly overestimate the cross-sections at the back-angle region. By matching the present theoretical calculations of the differential cross-sections with the experimental data, the spectroscopic factors in each reaction state are extracted

$$S(l,\, j) = \frac{1}{N_R} \frac{(2J_i + 1)}{(2J + 1)} \frac{(d\sigma/d\Omega)_{\text{exp}}}{(d\sigma/d\Omega)_{\text{theor}}} \tag{19}$$

where N_R is normalization factor and the remaining symbols carry their usual meaning. The obtained values of these factors are listed in Table III.

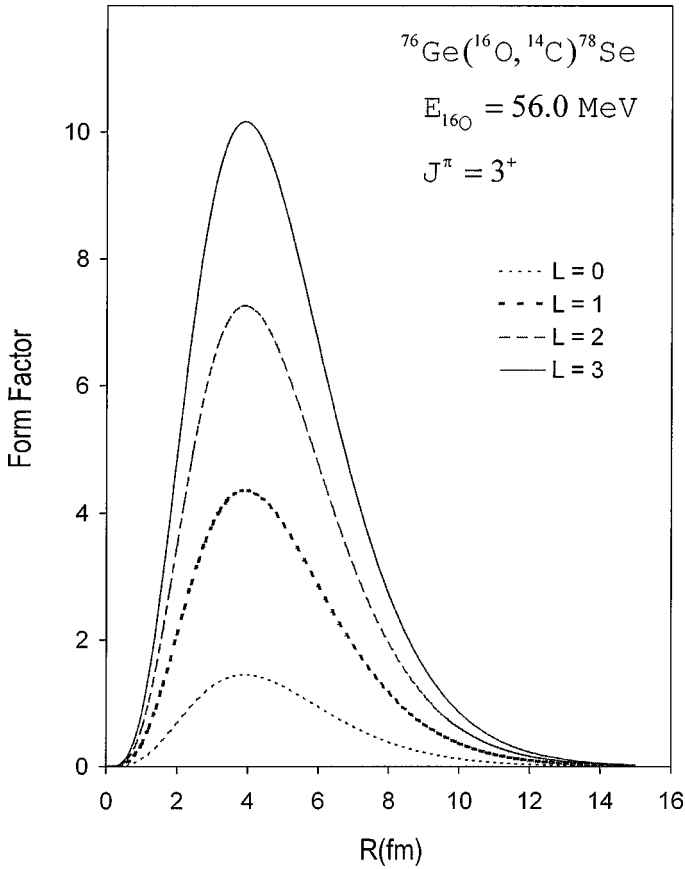

Fig. 2. Yukawa form factors of $^{76}Ge(^{16}O, ^{14}C)^{78}Se$ reaction for different angular momenta with optical potential parameters (Set I).

4. DISCUSSION AND CONCLUSIONS

In the present work, heavy-ion transfer reactions are successfully studied in the framework of the DWBA calculations employing different ion–ion interactions. The present calculations show that the form factors depend only on the value of the transferred angular momentum as shown in Figs. 1 and 2. The calculations of the angular distributions given in Figs. 3 and 4 show that the present DWBA calculations using real and imaginary Woods-Saxon potentials (WS + WS) reproduce the angular distributions in the forward angle region fairly well. Where calculations using J-dependent imaginary potential give an equivalent fit to the experimental data in the large angle region and introduce a description better than those using real and imaginary Woods-Saxon optical potential.

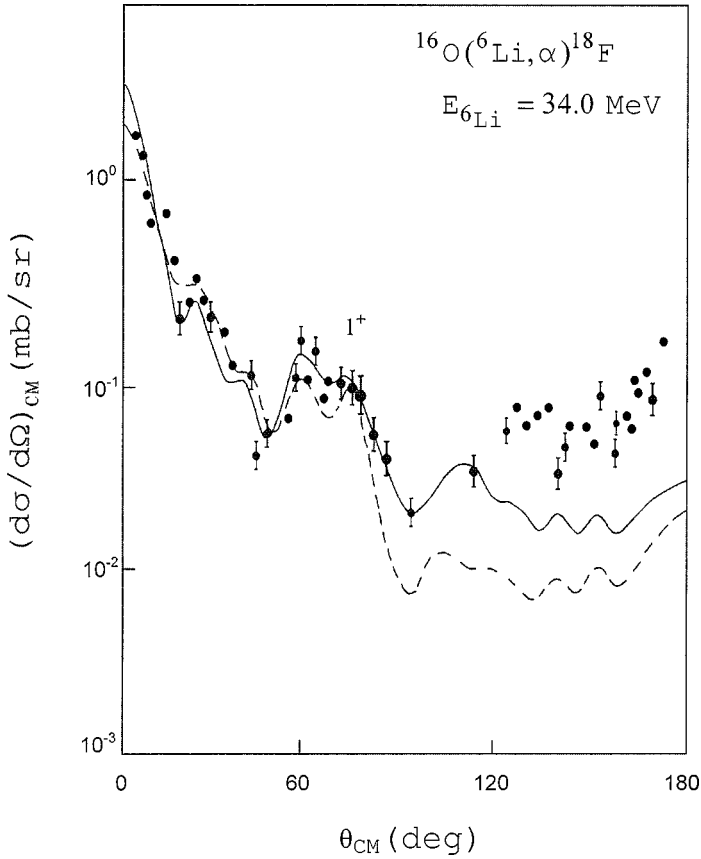

Fig. 3. Differential cross-sections of the $^{16}O(^{6}Li, \alpha)^{18}F$ two-nucleon transfer reaction (1^+, g.s.) at 34.0 MeV incident energy. The solid and dashed curves are the present theoretical DWBA calculations using (WS + JD) and (WS + WS) optical potentials, respectively. The dots are the experimental data taken from Ichihara and Yoshida (1986).

In general, the oscillatory structures of the calculated differential cross-sections at the forward angles are found to be unchanged with the choice of the optical potentials but those at large- and backward-angles are greatly affected. In addition, although the inclusion of the J-dependent term is found too small to account for the cross-section values at backward region, but it leads to better description than the Woods-Saxon potentials.

In conclusion, we conclude that both magnitudes and shapes of the differential cross-section are satisfactory well reproduced in the forward- and large-regions. Also, the present one-step DWBA calculations using real Woods-Saxon potential

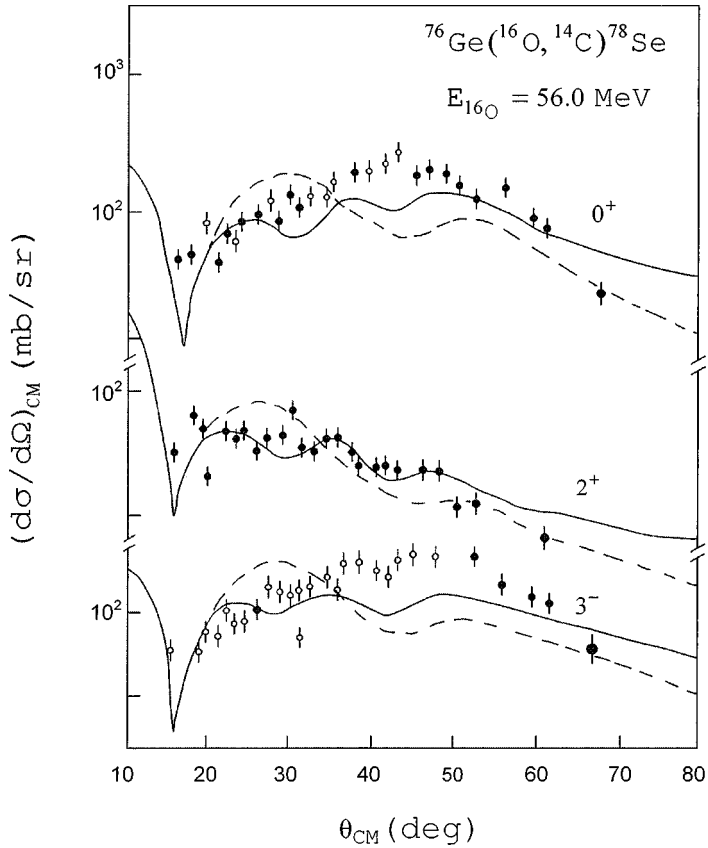

Fig. 4. The angular distribution of the $^{76}Ge(^{16}O, ^{14}C)^{78}Se$ two-nucleon transfer reaction at 56.0 MeV incident energy leading to 0.0, 0.61, and 2.50 MeV different ^{78}Se excited states. The solid and dashed curves are the present theoretical DWBA calculations using (WS + JD) and (WS + WS) optical potentials, respectively. The dots are the experimental data taken from Mermaz (1980).

Table III. Spectroscopic Factors

Reaction	Incident energy (MeV)	Excitation energy (MeV)	J^π	Previous	Present spectroscopic factors (WS + WS)	Present spectroscopic factors (WD + JD)
$^{16}O(^6Li, \alpha)^{18}F$	34.0	0.00	1^+	0.76	0.77	0.79
$^{76}Ge(^{16}O, ^{14}C)^{78}Se$	56.0	0.00	0^+	0.54	0.67	0.77
		0.61	2^+	0.62	0.71	0.79
		2.50	3^-	0.58	0.62	0.73

and imaginary J-dependent term are sufficient to describe the general features of two-nucleon transfer data.

REFERENCES

Bilwes, B., Bilwes, R., Stutige, L., Ballester, F., Diaz, J., Ferrero, J. L., Roldan, C., and Sanchez, F. (1987). *Nuclear Physics A* **473**, 353.

Charagi, S. K., Gupta, S. K., Betigeri, M. G., Fernandes, C. V., and Kauldeep. (1993). *Physical Review C* **48**, 1153.

Ferrero, J. L., Ruiz, J. A., Bilwes, B., and Bilwes, R. (1990). *Nuclear Physics A* **510**, 360.

Gao, C.-Q., Ning, P.-Z., and He, G.-Z. (1988). *Nuclear Physics A* **485**, 282.

Humanic, T. J., Ernst, H., Henning, W., and Zeidman, B. (1982). *Physical Review C* **26**, 993.

Ichihara, H. and Yoshida, H. (1986). *Nuclear Physics A* **448**, 546.

Kabir, A., Kermod, M. W., and Rowley, N. (1988). *Nuclear Physics A* **481**, 94.

Kondo, Y., Robson, B. A., Smith, R., and Wolter, H. H. (1985). *Physics Letters B* **162**, 39.

Kondo, Y. and Tamura, T. (1984). *Physical Review C* **30**, 97.

Lepine-Szily, A., Obuti, M. M., Lichtenthaler Filho, R., Oliveira, J. M., Jr., and Villari, A.C.C. (1990). *Physics Letters B* **243**, 23.

Maglione, E., Pollarolo, G., Vitturi, A., Broglia R. A., and Winther, A. (1985). *Physics Letters B* **162**, 59.

Mermaz, M. C. (1980). *Physical Review C* **21**, 2356.

Sikora, B., Blann, M., Bisphinghoff W., and Beckerman. (1980). *Physical Review C* **21**, 614.

Tamaura, T. (1974). *Physics Reports* **14**(2), 59.

Tanabe, T., Yasue, M., Sato, K., Ogino, K., Kadota, Y., Taniguchi, Y., Obori, K., Makino, K., Tochi, M., Mermaz, M. C., Auger F., and Fernandez, B. (1981). *Physical Review C* **24**, 2556.

Treka, D. E., Frawley, A. D., Kemper, K. W., Robson, D., Fex, J. D., and Myers, E. G. (1990). *Physical Review C* **41**, 2134.

Videbaek, F., Hansen, O., Nilsson, B. S., Flynn E. R., and Peng, J. C. (1985). *Nuclear Physics A* **433**, 441.

Xia, L.-H. and He, G.-Z. (1988). *Nuclear Physics A* **485**, 291.